

An Efficient Two Dimensional Multiple Real-Valued Sinusoidal Signal Frequency Estimation Algorithm

Prasad Kar Sambit and P. Palanisamy

Abstract In order to alleviate the effect of additive noise and to reduce the computational burden, we proposed a new computationally efficient cross-correlation based two-dimensional frequency estimation method for multiple real valued sinusoidal signals. Here the frequencies of both the dimensions are estimated independently with a one-dimensional (1-D) subspace-based estimation technique without eigendecomposition, where the null spaces are obtained through a linear operation of the matrices formed from the cross-correlation matrix between the received data. The estimated frequencies in both the dimensions are automatically paired. Simulation results show that the proposed method offers competitive performance when compared to existing approaches at a lower computational complexity. It has shown that proposed method perform well at low signal-to-noise ratio (SNR) and with a small number of snapshots.

Keywords 2-D frequency estimation · Sub-space based method: Real-valued sinusoidal model · Cross-correlation

P. K. Sambit (✉) · P. Palanisamy (✉)

Department of Electronics and Communication Engineering, National Institute of Technology, Trichy 620015, India
e-mail: sambitpk@gmail.com

P. Palanisamy
e-mail: palan@nitt.edu

1 Introduction

In this paper, we consider the problem of estimating the frequencies of multiple two-dimensional (2-D) real-valued sinusoids in presence of additive white Gaussian noise. This problem is the more precise case of estimating the parameters of a 2-D regular and homogeneous random field from a single observed realization as of [1]. The real-valued 2-D sinusoidal signal models, also known as X-texture modes. These modes come into existence naturally in experimental, analytical, modal and vibrational analysis of circular shaped objects. X-texture modes are often used for modelling the displacements in the cross-sectional planes of isotropic, homogeneous, thick walled cylinders [2–4], laminated composite cylindrical shells [5], and circular plates [6]. These X-texture modes have also been used to describe the radial displacements of logs of spruce subjected to continuous sinusoidal excitation [7] and standing trunks of spruce subjected to impact excitation [8–10]. The proposed signal model offers cumbersome challenges for 2-D joint frequency estimation algorithms. Many algorithms for estimating complex-valued frequencies are well documented in the literatures [11, 12] and for 1-D real-valued frequencies in [13–15]. A vivid discussion on the problem of analyzing 2-D homogeneous random fields with discontinuous spectral distribution functions can be found in [16]. Parameter estimation techniques of sinusoidal signals in additive white noise include the periodogram-based approximation (applicable for widely spaced sinusoids) to the maximum-likelihood (ML) solution [17–19], the Pisarenko harmonic decomposition [20], or the singular value decomposition [21]. A matrix enhancement and matrix pencil method for estimating the parameters of 2-D superimposed, complex-valued exponential signals was suggested in [11]. In [22], the concept of partial forward–backward averaging is proposed as a means for enhancing the frequency and damping estimation of 2-D multiple real-valued sinusoids (X-texturemodes) where each mode considered as a mechanism for forcing the two plane waves towards the mirrored direction-of-arrivals. In [23], 2-D parameter estimation of a single damped/undamped real/complex tone is proposed which is referred to as principal-singular-vector utilization for modal analysis (PUMA).

We present a new approach of solving the 2-D real valued sinusoidal signal frequencies estimation problem based on cross-correlation technique to resolve the identical frequencies. The proposed idea based upon the computationally efficient subspace based method without eigendecomposition (SUMWE) [24, 25]. The paper is organized as follows. The signal model, together with a definition of the addressed problem, is presented in Sect. 2. The basic definition and the proposed technique both are detailed in Sect. 3 followed by simulation results and conclusion in Sects. 4 and 5, respectively. Throughout this paper upper case, bold letters denote matrices where as lowercase bold letters are vectors. The superscript T denotes transposition of a matrix.

2 Data Model and Problem Definition

Consider the following set of noisy data:

$$r(m, n) = x(m, n) + e(m, n) \quad (1)$$

where $0 \leq m \leq N_1 - 1$ and $0 \leq n \leq N_2 - 1$. The model of the noiseless data $x(m, n)$ is described by,

$$x(m, n) = \sum_{k=1}^D a_k \cos(\omega_k m + \phi_{1k}) \cos(v_k n + \phi_{2k}) \quad (2)$$

The signal $x(m, n)$ consists of D , two dimensional real-valued sinusoids described by normalized 2-D frequencies $\{\omega_k, v_k\}$, ($k = 1, 2, \dots, D$), the real amplitude $\{a_k\}$ ($k = 1, 2, \dots, D$) and the phases ϕ_{1k} and ϕ_{2k} which are independent random variables uniformly distributed over $[0, 2\pi]$. $e(m, n)$ is a zero mean additive white Gaussian noise with variance σ^2 . Further assumed that α_k and β_k are independent of $e(m, n)$.

Let us define two $M \times 1$ snapshot vectors with assumption $M > D$, described as follows

$$\mathbf{y}_\omega(m, n) \triangleq \frac{1}{2} [\mathbf{y}_1(m, n) + \mathbf{y}_2(m, n)] \quad (3a)$$

$$\mathbf{y}_v(m, n) \triangleq \frac{1}{2} [\mathbf{y}_3(m, n) + \mathbf{y}_4(m, n)] \quad (3b)$$

where,

$$\mathbf{y}_1(m, n) \triangleq [r(m, n) \ r(m+1, n) \ \dots \ r(m+M-1, n)]^T \quad (4a)$$

$$\mathbf{y}_2(m, n) \triangleq [r(m, n) \ r(m-1, n) \ \dots \ r(m-M+1, n)]^T \quad (4b)$$

$$\mathbf{y}_3(m, n) \triangleq [r(m, n) \ r(m, n+1) \ \dots \ r(m, n+M-1)]^T \quad (4c)$$

$$\mathbf{y}_4(m, n) \triangleq, \text{left} [r(m, n) \ r(m, n-1) \ \dots \ r(m, n-M+1)]^T \quad (4d)$$

From the above set of equations we can obtain pair of expression for the two $M \times 1$ snapshot vectors by substituting equation (4a, b) in (3a) and (4c, d) in (3b) as follows,

$$y_\omega(m, n) = A(\omega)s(m, n) + g(m, n) \quad (5)$$

$$y_v(m, n) = A(v)s(m, n) + h(m, n) \quad (6)$$

where $A(\omega) = [\gamma(\omega_1) \ \dots \ \gamma(\omega_D)]$ and $A(v) = [\rho(v_1) \ \dots \ \rho(v_D)]$ are $M \times D$ matrices, and $s(m, n) = [a_1 \cos(\omega_1 m + \alpha_1) \cos(v_1 n + \beta_1) \ \dots \ a_D \cos(\omega_D m + \alpha_D) \cos(v_D n + \beta_D)]^T$ is the $D \times 1$ signal vector, $\gamma(\omega_i)$ and $\rho(v_i)$ are $M \times 1$ vectors defined respectively as

$\gamma(\omega_i)=[1 \cos(\omega_i)\dots\cos((M-1)\omega_i)]^T$ and $\rho(v_i)=[1 \cos(v_i)\dots\cos((M-1)v_i)]^T$. The modified $M \times 1$ error vectors $\mathbf{g}(m,n)$ and $\mathbf{h}(m,n)$ are defined respectively as $\mathbf{g}(m,n) \triangleq [g_1(m,n) g_2(m,n) \dots g_M(m,n)]^T$ and $\mathbf{h}(m,n) \triangleq [h_1(m,n) h_2(m,n) \dots h_M(m,n)]^T$, where $g_j(m,n) = 1/2[e(m+j-1,n) + e(m-j+1,n)]$ and $h_j(m,n) = 1/2[e(m,n+j-1) + e(m,n-j+1)]$. The matrices $\mathbf{A}(\omega)$ and $\mathbf{A}(v)$ are full rank matrices because all the columns are linearly independent to each other.

2.1 Data Model Modification

We first obtained two new data models as follows,

$$\mathbf{z}_\omega(m,n) = \mathbf{A}(\omega)\Omega_\omega\mathbf{s}(m,n) + \mathbf{q}_r(m,n) \quad (7)$$

$$\mathbf{z}_v(m,n) = \mathbf{A}(v)\Omega_v\mathbf{s}(m,n) + \mathbf{q}_c(m,n) \quad (8)$$

by implementing following mathematical operations,

$$z_\omega(m,n) = \frac{1}{4} \sum_{j=1}^4 z_j(m,n) \quad (9a)$$

$$\mathbf{z}_v(m,n) = \frac{1}{4} \sum_{j=5}^8 \mathbf{z}_j(m,n) \quad (9b)$$

where

$$\mathbf{z}_1(m,n) \triangleq [r(m+1,n) r(m,n) r(m-1,n) \dots r(m-M+2,n)]^T \quad (10a)$$

$$\mathbf{z}_2(m,n) \triangleq [r(m-1,n) r(m,n) r(m+1,n) \dots r(m+M-2,n)]^T \quad (10b)$$

$$\mathbf{z}_3(m,n) \triangleq [r(m-1,n) r(m-2,n) r(m-3,n) \dots r(m-M,n)]^T \quad (10c)$$

$$\mathbf{z}_4(m,n) \triangleq [r(m+1,n) r(m+2,n) r(m+3,n) \dots r(m+M,n)]^T \quad (10d)$$

$$\mathbf{z}_5(m,n) \triangleq [r(m,n+1) r(m,n) r(m,n-1) \dots r(m,n-M+2)]^T \quad (11a)$$

$$\mathbf{z}_6(m,n) \triangleq [r(m,n-1) r(m,n) r(m,n+1) \dots r(m,n+M-2)]^T \quad (11b)$$

$$\mathbf{z}_7(m,n) \triangleq [r(m,n-1) r(m,n-2) r(m,n-3) \dots r(m,n-M)]^T \quad (11c)$$

$$\mathbf{z}_8(m,n) \triangleq [r(m,n+1) r(m,n+2) r(m,n+3) \dots r(m,n+M)]^T \quad (11d)$$

where $z_i(m,n)$ for $i = 1,2,\dots,8$ are $M \times 1$ observation vectors. Ω_ω and Ω_v are two $D \times D$ diagonal matrices defined respectively as $\Omega_\omega = \text{diag}\{\cos\omega_1 \dots \cos\omega_D\}$ and $\Omega_v = \text{diag}\{\cos v_1 \dots \cos v_D\}$. The two $M \times 1$ modified noise vectors $\mathbf{q}_r(m,n)$ and

$q_e(m,n)$ are defined respectively as $q_r(m,n) = [q_{r1}(m,n) \dots q_{rM}(m,n)]^T$, $q_e(m,n) = [q_{e1}(m,n) \quad q_{e2}(m,n) \dots q_{eM}(m,n)]^T$ where $q_{ri}(m,n) = 1/4[e(m-i+2,n) + e(m+i-2,n) + e(m+i,n) + e(m-i,n)]$ and $q_{ei}(m,n) = 1/4[e(m,n-i+2) + e(m,n+i-2) + e(m,n+i) + e(m,n-i)]$ for $i = 1, 2, \dots, M$.

2.2 Further Modification of Data Model

As like Sect. 2.1, we deduced another set of modified data models described by,

$$\mathbf{p}_\omega(m,n) = \mathbf{JA}(\omega)\Omega_\omega \mathbf{s}(m,n) + \mathbf{q}_w(m,n) \quad (12)$$

$$\mathbf{p}_v(m,n) = \mathbf{JA}(v)\Omega_v \mathbf{s}(m,n) + \mathbf{q}_u(m,n) \quad (13)$$

The above two data models were obtained by implementing similar kind of mathematical operations as that of equation (9a, b) that is,

$$\mathbf{p}_\omega(m,n) = \frac{1}{4} \sum_{j=1}^4 \mathbf{p}_j(m,n) \quad (14)$$

$$\mathbf{p}_v(m,n) = \frac{1}{4} \sum_{j=5}^8 \mathbf{p}_j(m,n) \quad (15)$$

where

$$\mathbf{p}_1(m,n) \triangleq [r(m-M+2,n) \dots r(m-1,n) \quad r(m,n) \quad r(m+1,n)]^T \quad (16a)$$

$$\mathbf{p}_2(m,n) \triangleq [r(m+M-2,n) \dots r(m+1,n) \quad r(m,n) \quad r(m-1,n)]^T \quad (16b)$$

$$\mathbf{p}_3(m,n) \triangleq [r(m-M,n) \dots r(m-3,n) \quad r(m-2,n) \quad r(m-1,n)]^T \quad (16c)$$

$$\mathbf{p}_4(m,n) \triangleq [r(m+M,n) \dots r(m+3,n) \quad r(m+2,n) \quad r(m+1,n)]^T \quad (16d)$$

$$\mathbf{p}_5(m,n) \triangleq [r(m,n-M+2) \dots r(m,n-1) \quad r(m,n) \quad r(m,n+1)]^T \quad (17a)$$

$$\mathbf{p}_6(m,n) \triangleq [r(m,n+M-2) \dots r(m,n+1) \quad r(m,n) \quad r(m,n-1)]^T \quad (17b)$$

$$\mathbf{p}_7(m,n) \triangleq [r(m,n-M) \dots r(m,n-3) \quad r(m,n-2) \quad r(m,n-1)]^T \quad (17c)$$

$$\mathbf{p}_8(m,n) \triangleq [r(m,n+M) \dots r(m,n+3) \quad r(m,n+2) \quad r(m,n+1)]^T \quad (17d)$$

where $\mathbf{p}_i(m,n)$ for $i = 1, 2, \dots, 8$ are $M \times 1$ observation vectors and \mathbf{J} is the $M \times M$ counter identity matrix, in which 1 s present in the principal anti-diagonal. The two $M \times 1$ modified noise vectors $\mathbf{q}_w(m,n)$ and $\mathbf{q}_u(m,n)$ are defined respectively as $\mathbf{q}_w(m,n) = \mathbf{J}q_r(m,n)$ and $\mathbf{q}_u(m,n) = \mathbf{J}q_e(m,n)$.

3 Proposed Algorithm

In this section, we present the algorithm for 2-D frequency estimation for multiple real-valued sinusoidal signals.

3.1 Estimation of First Dimension Frequencies

Under the assumption of data model, from (5) and (7) we easily obtain the cross correlation matrix \mathbf{R}_{yz1} between the received data, $y_\omega(m,n)$ and $z_\omega(m,n)$ as,

$$\mathbf{R}_{yz1} = E\{y_\omega(m,n)\mathbf{z}_\omega^T(m,n)\} = \mathbf{A}(\omega)\mathbf{R}_{ss}\mathbf{\Omega}_\omega\mathbf{A}^T(\omega) \quad (18)$$

where \mathbf{R}_{ss} is source signal correlation matrix defined by $\mathbf{R}_{ss} \triangleq E\{\mathbf{s}(m,n)\mathbf{s}^T(m,n)\}$. From (12), we have another data model that is $p_\omega(m,n)$ in backward way such that $p_\omega(m,n) = Jz_\omega(m,n)$, similarly from (5) and (12) we can obtain another cross-correlation matrix between the two received data

$$\mathbf{R}_{yp1} = E\{y_\omega(m,n)\mathbf{p}_\omega^T(m,n)\} = \mathbf{A}(\omega)\mathbf{R}_{ss}\mathbf{J}\mathbf{\Omega}_\omega\mathbf{A}^T(\omega) \quad (19)$$

In noise free case $\mathbf{R}_{yp1} = \mathbf{J}\mathbf{R}_{yz1}$ but in practical case that is when signal is noise corrupted, then the relation holds true partially that is $\mathbf{R}_{yp1} \cong \mathbf{J}\mathbf{R}_{yz1}$. Considering the above assumptions we formulated an extended cross correlation of size $M \times 2M$ as,

$$\mathbf{R}_\omega = [\mathbf{R}_{yz1}\mathbf{R}_{yp1}] = [\mathbf{R}_{yz1}\mathbf{J}\mathbf{R}_{yz1}] = \mathbf{A}(\omega)[\mathbf{R}_{ss}\mathbf{\Omega}_\omega\mathbf{A}^T(\omega)\mathbf{R}_{ss}\mathbf{J}\mathbf{\Omega}_\omega\mathbf{A}^T(\omega)] \quad (20)$$

Since $\mathbf{A}(\omega)$ is a full rank matrix, we can divide $\mathbf{A}(\omega)$ into two sub matrices as $\mathbf{A}(\omega) = [(\mathbf{A}_1(\omega))^T (\mathbf{A}_2(\omega))^T]^T$ where $\mathbf{A}_1(\omega)$ and $\mathbf{A}_2(\omega)$ are the $D \times D$ and $(M-D) \times D$ sub matrices consisting of the first D rows and last $(M-D)$ rows of the matrix $\mathbf{A}(\omega)$ respectively. There exists a $D \times M-D$ linear operator \mathbf{P}_1 between $\mathbf{A}_1(\omega)$ and $\mathbf{A}_2(\omega)$ [26] such that $\mathbf{A}_2(\omega) = \mathbf{P}_1^T\mathbf{A}_1(\omega)$, using the above assumptions we can segregate (20) into the following two matrices.

$$\begin{aligned} \mathbf{R}_\omega &= [(\mathbf{A}_1(\omega))^T (\mathbf{A}_2(\omega))^T]^T [\mathbf{R}_{ss}\mathbf{\Omega}_\omega\mathbf{A}^T(\omega)\mathbf{R}_{ss}\mathbf{J}\mathbf{\Omega}_\omega\mathbf{A}^T(\omega)] \\ &= [(\mathbf{A}_1(\omega))^T \mathbf{P}_1^T \mathbf{A}_1(\omega)]^T [\mathbf{R}_{ss}\mathbf{\Omega}_\omega\mathbf{A}^T(\omega)\mathbf{R}_{ss}\mathbf{J}\mathbf{\Omega}_\omega\mathbf{A}^T(\omega)] \\ &\triangleq [\mathbf{R}_{\omega 1}^T \mathbf{R}_{\omega 2}^T]^T \end{aligned} \quad (21)$$

where $\mathbf{R}_{\omega 1}$ and $\mathbf{R}_{\omega 2}$ consist of the first D rows and the last $M-D$ rows of the matrix \mathbf{R}_ω , and $\mathbf{R}_{\omega 2} = \mathbf{P}_1^T \mathbf{R}_{\omega 1}$. Hence, the linear operator \mathbf{P}_1 found from $\mathbf{R}_{\omega 1}$ and $\mathbf{R}_{\omega 2}$ as [26]. However, a least-squares solution [27] for the entries of the propagator matrix \mathbf{P}_1 satisfying the relation, $\mathbf{R}_{\omega 2} = \mathbf{P}_1^T \mathbf{R}_{\omega 1}$ obtained by minimizing the cost function described as follows,

$$\zeta(\mathbf{P}_1) = \|\mathbf{R}_{\omega_2} - \mathbf{P}_1^T \mathbf{R}_{\omega_1}\|^2 \quad (22)$$

where $\|\cdot\|_F^2$ denotes the Frobenius norm. The cost function $\zeta(\mathbf{P}_1)$ is a quadratic (convex) function of \mathbf{P}_1 , which can be minimized to give the unique least-square solution for \mathbf{P}_1 , that can be evidently shown as,

$$\mathbf{P}_1 = (\mathbf{R}_{\omega_1} \mathbf{R}_{\omega_1}^T)^{-1} \mathbf{R}_{\omega_1} \mathbf{R}_{\omega_2}^T \quad (23)$$

further by defining another matrix $\mathbf{Q}_\omega = [P_1^T - I_{M-D}]^T$, such that $\mathbf{Q}_\omega^T \mathbf{A}(\omega) = \mathbf{0}_{(M-D) \times D}$ which can be used to estimate the real valued harmonic frequencies of first dimension $\{\omega_k\}$ for $k = 1, 2, \dots, D$ as like [25]. Thus when the number of snapshots are finite the frequencies of first dimension can be estimated by minimizing following cost function, $\hat{f}(\omega) = a^T(\omega) \hat{E} a(\omega)$ where $a(\omega) = [1 \cos \omega \dots \cos(M-1)\omega]^T$ and $\hat{E} \triangleq \hat{\mathbf{Q}}_\omega (\hat{\mathbf{Q}}_\omega^T \hat{\mathbf{Q}}_\omega)^{-1} \hat{\mathbf{Q}}_\omega^T$. The orthonormality of matrix $\hat{\mathbf{Q}}_\omega$ is used in order to improve the estimation performance while \mathbf{E} is calculated implicitly using matrix inversion lemma as [24] and \hat{E} and $\hat{\mathbf{Q}}_\omega$ are the estimates of \mathbf{E} and \mathbf{Q}_ω .

Steps for estimating ω_k :

- Calculate the estimate \hat{R}_ω of the cross-correlation matrix \mathbf{R}_ω using (20).
- Partition \hat{R}_ω and determine \hat{R}_{ω_1} and \hat{R}_{ω_2} .
- Determine the estimate of the propagator matrix \mathbf{P}_1 using (23).
- Define $\hat{\mathbf{Q}}_\omega = [\hat{P}_1^T - I_{M-D}]^T$ and from $\hat{\mathbf{Q}}_\omega$ find out $\hat{E} \triangleq \hat{\mathbf{Q}}_\omega (\hat{\mathbf{Q}}_\omega^T \hat{\mathbf{Q}}_\omega)^{-1} \hat{\mathbf{Q}}_\omega^T$ using matrix inversion lemma.
- The first dimension frequencies that is, $\{\omega_k\}$ for $k = 1, 2, \dots, D$ estimated by minimizing the following cost function, $\hat{f}(\omega) = a^T(\omega) \hat{E} a(\omega)$.

3.2 Estimation of Second Dimension Frequencies

The method adopted for estimating the first dimension frequencies ω_i for $i = 1, 2, \dots, D$, can be used for estimating the second dimension frequencies ν_i for $i = 1, 2, \dots, D$. That is the same procedure used in Sect. 3.1 of this Section applied to estimate second dimension frequencies. The second dimension frequencies obtained by doing similar kind of operation across the data models developed in (6), (8) and (13).

The proposed method has notable advantages over the conventional MUSIC algorithm [15], such as computational simplicity and less restrictive noise model. Though it required peak search but there is no eigenvalue decomposition (SVD or EVD) involved in the proposed algorithm unlikely MUSIC, where the EVD of the auto correlation matrix is needed. It also provide quite efficient estimate of the

frequencies and the estimated frequencies in both dimensions are automatically paired.

4 Simulation Results

Computer simulation have been carried out to evaluate the frequency estimation performance of the proposed algorithm for 2-D multiple real-valued sinusoids in presence of additive white Gaussian noise. The average root-mean-square-error (RMSE) is employed as performance measure, apart from that some other simulations also conducted to show the detection capability and bias of estimation. Besides CRLB, the performance of the proposed algorithm is compared with those of 2D-MUSIC and 2D-ESPRIT [28] algorithms for real-valued sinusoids. Four type of analysis have been performed.

4.1 Analysis of Frequency Spectra

The signal parameters are $N_1 = N_2 = 50$ and the dimension of snapshot vector $M = 20$. Number of undamped 2-D real-valued sinusoids $D = 2$, amplitude $\{a_k = 1\}$ for $k = 1, 2, \dots, D$. The first dimension frequencies, and the second dimension frequencies are $(\omega_1, \omega_2) = (0.1\pi, 0.13\pi)$ and $(\nu_1, \nu_2) = (0.13\pi, 0.16\pi)$ respectively. Note that the frequency separation is 0.03, which is smaller than the Fourier resolution capacity $1/M (=0.05)$. This means classic FFT-based method cannot resolve these two frequencies, and also this method can resolve identical frequencies present in different dimensions ($\omega_2 = \nu_1 = 0.13\pi$). Figure 1 displays spectra of the proposed algorithm at SNR = 10 dB. We can see from Fig. 1 that the frequency parameters in both the dimensions are accurately resolved. The estimated frequencies are shown in Table 1.

In second analysis that is shown in Fig. 2 where we considered the signal parameters are $N_1 = N_2 = 100$ and the dimension of snapshot vector $M = 50$, keeping all other parameters same as previous experiment. The detection of frequencies in both the dimensions are found to be more accurate. The estimated frequencies of this analysis are shown in Table 2.

4.2 Performance Analysis Considering RMSE

The same signal parameters as first analysis of Sect. 4.1 of this section is considered. We compared root-mean-square-error (RMSE) on the estimates for the proposed algorithm, MUSIC and 2-D ESPRIT algorithm as a function of SNR. Here a Monte-Carlo simulation of 500 runs was performed. Figure 3a shows the

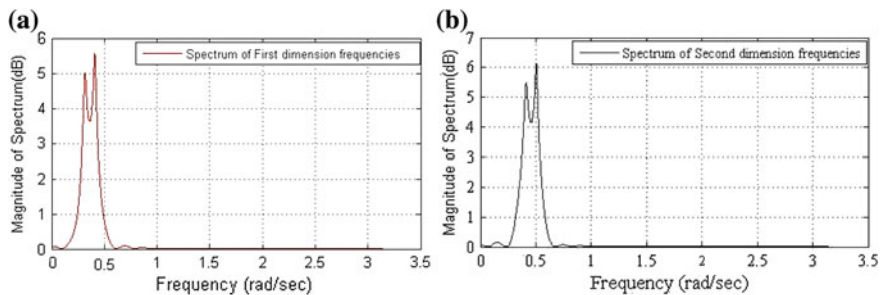


Fig. 1 Spectrum of frequencies in both dimensions ($M = 20$)

Table 1 Estimated frequencies considering $M = 20$

Frequency	Original frequency(rad/sec)	Estimated frequency(rad/sec)
ω_1	0.1π	0.1012π
ω_2	0.13π	0.1285π
ν_1	0.13π	0.1289π
ν_2	0.16π	0.1594π

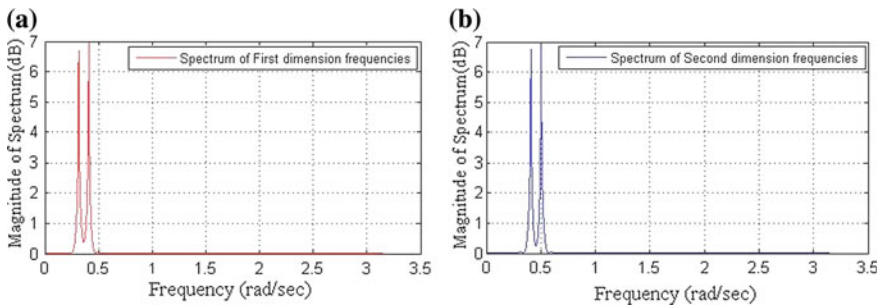


Fig. 2 Spectrum of frequencies in both dimensions ($M = 50$)

Table 2 Estimated frequencies considering $M = 50$

Frequency	Original frequency(rad/sec)	Estimated frequency(rad/sec)
ω_1	0.1π	0.1003π
ω_2	0.13π	0.1303π
ν_1	0.13π	0.1303π
ν_2	0.16π	0.1604π

RMSEs and the corresponding CRB of first 2-D frequencies $\{\omega_k\}$, while Fig. 3b shows the second 2-D frequencies $\{\nu_k\}$ ($k = 1, 2, \dots, D$). It is clearly seen that the proposed algorithm outperforms the ESPRIT algorithm and in lower SNR case the

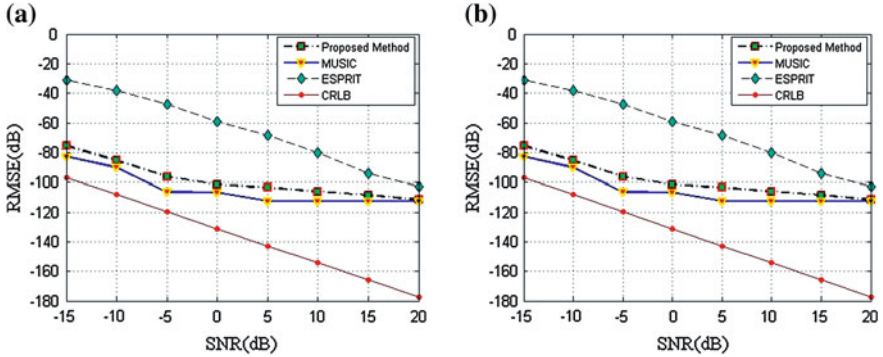


Fig. 3 **a** RMSE (dB) for first dimension frequencies vs SNRs (dB). **b** RMSE (dB) for second dimension frequencies vs SNRs (dB)

performance is similar to that of MUSIC algorithm. As SNR increases the proposed algorithm performs exactly same as that of MUSIC algorithm.

4.3 Performance Analysis Considering Probability of Correct Estimation and Bias of Estimation

In this analysis, we considered Probability of correct estimation of frequencies as performance measure. Taking the same signal parameters as of last two Sections, we determined the probability of correct estimation of 2-D real-valued sinusoidal signal frequencies for both dimensions by varying SNR. The obtained results are shown in Fig. 4a, b. From the above analysis, it is evident that proposed method performs far superior compared to 2-D ESPRIT and behaves in a same way as conventional MUSIC algorithm but without any eigendecomposition (EVD/SVD). Similarly we analyzed the bias of estimation for each dimensions and the results are plotted in Fig. 5a, b respectively. From bias analysis, it is clear that the proposed method performs much better than ESPRIT and almost similar to that conventional MUSIC algorithm in varied SNR ranges.

4.4 Performance Analysis Considering Computational Time

In this section we compared the performance of proposed method and conventional MUSIC algorithm based on their computational timing. Considering the same signal parameters at a fixed SNR of 10 dB we vary the snapshot vector dimension (M) and the results are plotted in Fig. 6. From Fig. 6 its clear that proposed method is less time consuming compared to conventional MUSIC algorithms.

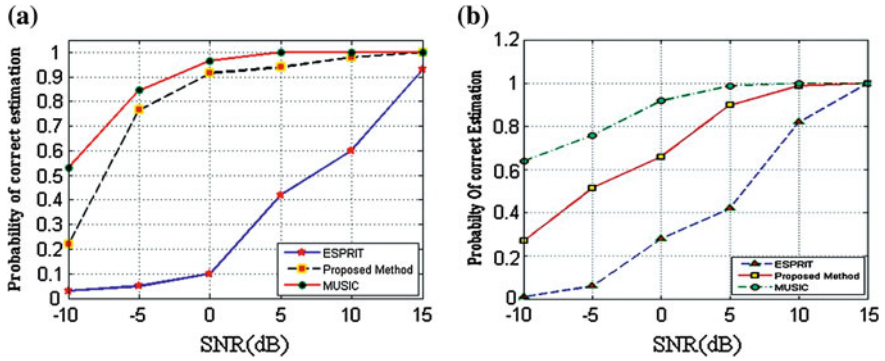


Fig. 4 a Probability of correct estimation for first dimension frequencies vs SNRs (dB). b Probability of correct estimation for second dimension frequencies vs SNRs (dB)

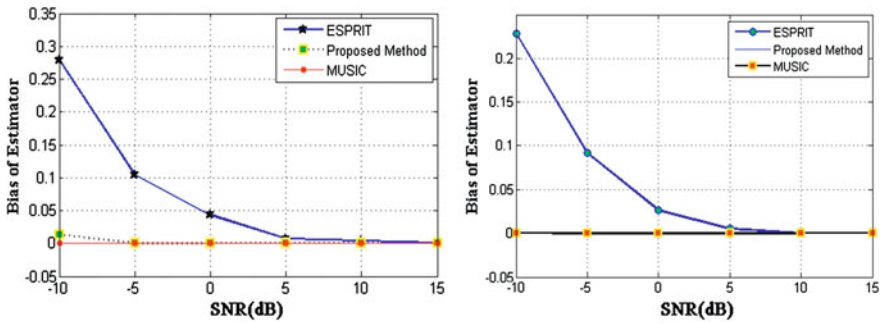
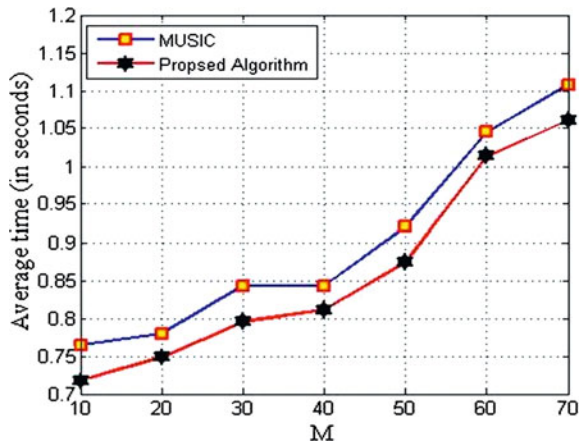


Fig. 5 a Bias of the estimator for first dimension frequencies vs SNR's (dB). b Bias of the estimator for second dimension frequencies vs SNR's (dB)

Fig. 6 Average computational time vs M at SNR = 10 dB



5 Conclusion

We have proposed a new approach based on subspace method without eigendecomposition using cross-correlation matrix for estimation of multiple real-valued 2-D sinusoidal signal frequencies embedded with additive white Gaussian noise. We have analytically quantified the performance of the proposed algorithm. It is shown that our algorithm remains operational when there exist identical frequencies in both the dimensions. Simulation results show that the proposed algorithm offers comparative performance when compared to MUSIC algorithm, but at a lower computational complexity and exhibit far superior performance when compared to ESPRIT algorithm. The frequency estimates thus obtained are automatically paired without an extra pairing algorithm.

References

1. Francos JM, Friedlander B (1998) Parameter estimation of two-dimensional moving average random fields. *IEEE Trans Signal Process* 46:2157–2165
2. Wang H, Williams K (1996) Vibrational modes of cylinders of finite length. *J Sound Vib* 191(5):955–971
3. Verma S, Singal R, Williams K (1987) Vibration behavior of stators of electrical machines, part I: theoretical study. *J Sound Vib* 115(1):1–12
4. Singal R, Williams K, Verma S (1987) Vibration behavior of stators of electrical machines, part II: experimental study. *J Sound Vib* 115(1):13–23
5. Zhang XM (2001) Vibration analysis of cross-ply laminated composite cylindrical shells using the wave propagation approach. *Appl Acoust* 62:1221–1228
6. So J, Leissa A (1998) Three-dimensional vibrations of thick circular and annular plates. *J Sound Vib* 209(1):15–41
7. Skatter S (1996) TV holography as a possible tool for measuring transverse vibration of logs: a pilot study. *Wood Fiber Sci* 28(3):278–285
8. Axmon J, Hansson M (1999) Estimation of circumferential mode parameters of living trees. In: *Proceedings of the IASTED international conference on signal image process (SIP'99)*, pp 188–192
9. Axmon J (2000) On detection of decay in growing norway spruce via natural frequencies. *Licentiate of Engineering Thesis Lund University*. Lund, Sweden, Oct 2000
10. Axmon J, Hansson M, Sörnmo L (2002) Modal analysis of living spruce using a combined Prony and DFT multichannel method for detection of internal decay. *Mech Syst Signal Process* 16(4):561–584
11. Hua Y (1992) Estimating two-dimensional frequencies by matrix enhancement and matrix pencil. *IEEE Trans Signal Process* 40(9):2267–2280
12. Haardt M, Roemer F, DelGaldo G (2008) Higher-order SVD-based subspace estimation to improve the parameter estimation accuracy in multidimensional harmonic retrieval problems. *IEEE Trans Signal Process* 56(7):3198–3213
13. Mahata K (2005) Subspace fitting approaches for frequency estimation using real-valued data. *IEEE Trans Signal process* 53(8):3099–3110
14. Palanisamy P, Sambit PK (2011) Estimation of real-valued sinusoidal signal frequencies based on ESPRIT and propagator method. In: *Proceedings of the IEEE-international conference on recent trends in information technology*, pp 69–73 June 2011

15. Stoica P, Eriksson A (1995) MUSIC estimation of real-valued sine-wave frequencies. *Signal process* 42(2):139–146
16. Priestley MB (1981) *Spectral analysis and time series*. Academic, New York
17. Walker M (1971) On the estimation of a harmonic component in a time series with stationary independent residuals. *Biometrika* 58:21–36
18. Rao CR, Zhao L, Zhou B (1994) Maximum likelihood estimation of 2-D superimposed exponential signals. *IEEE Trans Signal Process* 42:1795–1802
19. Kundu D, Mitra A (1996) Asymptotic properties of the least squares estimates of 2-D exponential signals. *Multidim Syst Signal Process* 7:135–150
20. Lang SW, McClellan JH (1982) The extension of Pisarenko’s method to multiple dimensions. In: *Proceedings of the international conference on acoustics, speech, and signal processing*, pp 125–128
21. Kumaresan R, Tufts DW (1981) A two-dimensional technique for frequency wave number estimation. *Proc IEEE* 69:1515–1517
22. Axmon J, Hansson M, Sörnmo L (2005) Partial forward–backward averaging for enhanced frequency estimation of real X-texture modes. *IEEE Trans Signal Process* 53(7):2550–2562
23. So HC, Chan FKW, Chan CF (2010) Utilizing principal singular vectors for two-dimensional single frequency estimation. In: *Proceedings of the IEEE international conference on acoustics, speech, signal process*, pp 3882–3886, March 2010
24. Xin J, Sano A (2004) Computationally efficient subspace-based method for direction-of-arrival estimation without eigen decomposition. *IEEE Trans Signal process* 52(4):876–893
25. Sambit PK, Palanisamy P (2012) A propagator method like algorithm for estimation of multiple real-valued sinusoidal signal frequencies. *Int J Electron Electr Eng* 6:254–258
26. Marcos S, Marsal A, Benidir M (1995) The propagator method for source bearing estimation. *Signal Process* 42(2):121–138
27. Golub GH, Van Loan CF (1980) An analysis of the total least squares problem. *SIAM J Numer Anal* 17:883–893
28. Rouquette S, Najim M (2001) Estimation of frequencies and damping factors by two-dimensional ESPRIT type methods. *IEEE Trans Signal Process* 49(1):237–245